IEEE Access
Multidisciplinary | Rapid Review | Open Access Journal

Received 26 November 2022, accepted 19 December 2022, date of publication 5 January 2023, date of current version 10 January 2023.

Digital Object Identifier 10.1109/ACCESS.2023.3234255

APPLIED RESEARCH

Input Spectrum Design for Identification of a Thermostat System

MD. TANJIL SARKER[1], AI HUI TAN[1], AND TIMOTHY TZEN VUN YAP[2]
[1]Faculty of Engineering, Multimedia University, Cyberjaya 63100, Malaysia
[2]Faculty of Computing and Informatics, Multimedia University, Cyberjaya 63100, Malaysia

Corresponding author: Ai Hui Tan (htai@mmu.edu.my)

This work was supported by the Multimedia University, Malaysia, under the Graduate Research Assistantship Scheme and Information and Communication Technology (ICT) Division, Bangladesh, under the ICT Research Fellowship Scheme.

ABSTRACT This paper considers the shaping of the amplitude spectra of perturbation signals for the identification of a thermostat system. The current approach in control engineering practice utilizes flat spectrum signals, which may not result in the highest possible accuracy. This research aims to investigate the effectiveness of optimal signals with amplitude spectra designed using two state-of-the-art software approaches, namely the model-based optimal signal excitation 2 (MOOSE2) design and the optimal excitation (optexcit) design, in improving estimation accuracy. Such a comparison on a real system is currently lacking. In particular, there exists a research gap on how the combined choice of signal and model structure affects performance measures. In this research, two model structures are used, which are the autoregressive with exogenous input (ARX) and the output error (OE) model structures. Four performance measures are compared, namely the determinant of the covariance matrix of the parameter estimates and the minimum error, mean error and maximum error in the frequency response. Results show that the optimal signals are effective in reducing the determinant of the covariance matrix and the maximum error in the frequency response for the thermostat system, when applied in combination with the ARX model structure. The flat spectrum signal remains very useful as a general broadband perturbation signal as it provides a good overall fit of the frequency response. The findings from this work highlight the benefits of applying optimal signals especially if the identification results are to be used for control, since these signals improve key performance measures which have direct implications on controller design.

INDEX TERMS Estimation, perturbation signals, signal design, system identification, thermostat systems.

I. INTRODUCTION

System identification is widely applied in control engineering to build models from input-output data [1]. These models are particularly useful in the design of model-based controllers such as the model predictive controller [2]. The accuracy of the model depends on the quality of the input-output data which is, in turn, determined by the input or perturbation signal used for the identification test. Periodic perturbation signals have the advantages of allowing the effects of transients to be removed and enabling averaging to be performed [3]. They can be categorized into fixed spectrum and computer-optimized signals [4]. The former category is constructed based on finite field arithmetic, whereas the latter category is generated via optimization using computer programs [5]. One of the characteristics that can be optimized is the amplitude spectrum.

Flat spectrum signals are ideal when there is little prior information available about the system under test. However, they may not result in the highest possible estimation accuracy. Fortunately, in some cases, such as in model predictive control applications, an initial model of the system is available at the point when an updated model is sought after due to process aging and revamps. In many other applications, it is possible to extract information about the system under test from historical data or preliminary step tests. It is useful to

The associate editor coordinating the review of this manuscript and approving it for publication was Taous Meriem Laleg-Kirati.

capitalize on the *a priori* information when designing perturbation signals since it is known that for the identification of linear systems, the asymptotic properties of the model parameter estimates depend only on the input spectrum [6]. Such signals are termed optimal signals. It is important to investigate how their amplitude spectra affect performance measures related to estimation accuracy since this will determine the usability of the models obtained.

Several signal designs are available in the literature, such as [7], [8], [9], [10], [11], [12], [13], and [14]. In [7], signal design for non-iterative direct data-driven techniques was considered for data-driven control, where the amplitude spectrum was designed to minimize the degradation caused by noise. An online method using past input-output data was presented in [8], where it was shown to be sample efficient. In [9], two signal design criteria involving sensitivity functions were proposed and analyzed for the identification of systems with uncertainties. The approach in [10] viewed the signal design from the perspective of optimizing an input trajectory that maximizes parameter identifiability. The signal-to-noise ratio (SNR) was utilized to guide the amplitude spectrum shaping in [11]. Signal design for kernel-based identification was considered in [12], where a two-step procedure using quadratic transformation was applied. A Bayesian A-optimality method was proposed in [13], which can be utilized for online signal design, also in the context of kernel-based identification. More recently, the direct spectrum shaping technique [14] was proposed, with the advantage of having a significantly lower computational load compared to that of the Bayesian A-optimality approach.

Of the several designs available, those that come with user-friendly software implementations are particularly useful. Two of these software approaches represent the current state-of-the-art, namely the model-based optimal input signal design 2 (MOOSE2) from the MOOSE2 program [15], [16], [17] and the optimal excitation (optexcit) design from the Frequency Domain System Identification (FDIDENT) Toolbox in MATLAB [18], [19], [20], [21]. The improvement achieved in the estimation accuracy across an iteration for the optexcit signal was analyzed in [22] under various SNRs. In [23], the combined use of MOOSE2 and optexcit signals for the multivariable case was investigated, but the results are applicable only to the specific systems tested.

Despite several signal designs being available, there is a lack of comparison between them because different signals were typically tested on different systems in the literature, making comparison challenging. Additionally, the majority of the existing works deal only with simulated systems. This motivates the current work, where the input spectrum design is implemented on a thermostat system. In particular, the MOOSE2 and optexcit designs are compared with the benchmark flat spectrum signal. The results reveal how the combined choice of signal and model structure affects performance measures related to estimation accuracy. A thermostat system is used in this study for the following reasons. Firstly, the regulatory function of a thermostat can minimize energy consumption and provide cost savings of greater than 40% [24]. Secondly, the thermostat is rather ubiquitous, being used in air conditioners, water heaters, refrigerators and ovens, thus ensuring that the results of this research are very much applicable to control engineering practice. Thirdly, many thermodynamic systems such as furnaces [25] share similar characteristics in terms of the smoothness of the dynamic responses, allowing the findings from the current work to be generalized to a wide range of systems.

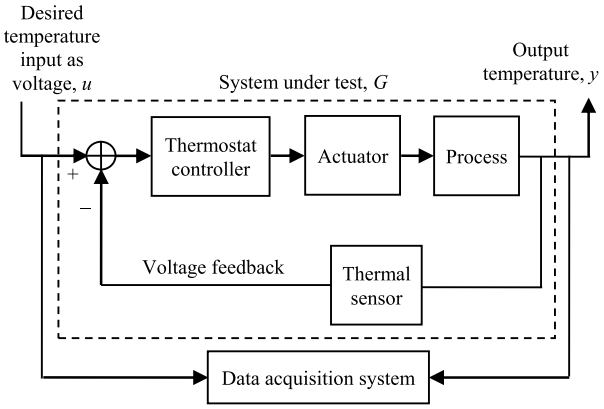

FIGURE 1. Block diagram of a thermostat system.

The rest of the paper is organized as follows. Section II provides the problem statement. Section III describes the experimental set-up. Preliminary tests and the identification of a benchmark model are described in Sections IV and V, respectively. Comparison between various signal designs is discussed in Section VI. Finally, concluding remarks and suggestions for future work are presented in Section VII.

II. PROBLEM STATEMENT

The block diagram of a general thermostat system is depicted in Figure 1. There are many types of thermostats available [24], which are suited for different applications. The controller may range from a simple on-off controller to a more complicated proportional-integral-derivative class of controller. The actuator depends on the heating and/or cooling mechanisms used and may range from a valve to a pulse-width modulator.

In this paper, the identification of the system under test is considered, where the input (denoted by u) is the desired temperature scaled to its corresponding voltage value and the output (denoted by y) is the temperature of the thermodynamic process. The perturbation signal is fed into the system as the input in order to excite the system. The problem statement is formally stated as follows. It is required to compare the estimation accuracy of the system transfer function $G(z) = Y(z)/U(z)$ for the flat, MOOSE2 and optexcit amplitude spectra, where U and Y denote the z-transforms of u and y, respectively, based on four performance measures:

(i) the determinant of the covariance matrix of the parameter estimates defined by

$$D = \det\{P\} \tag{1}$$

where P is the covariance matrix of the estimated parameters,

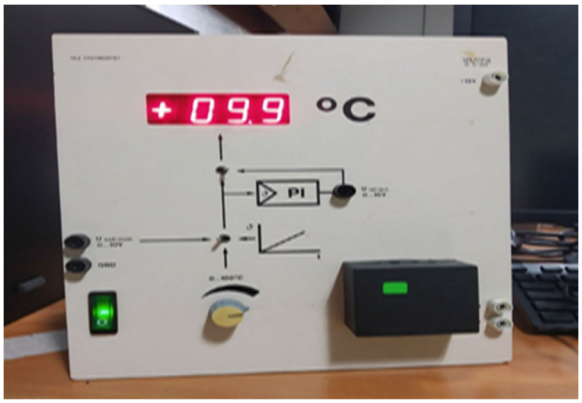

FIGURE 2. Photograph of ELWE LEHRSYSTEM thermostat.

(ii) the minimum error in the frequency response defined by

$$A_{\min} = \min_k (|\hat{G}(k) - G(k)|) \tag{2}$$

where $G(k)$ is the actual system frequency response and $\hat{G}(k)$ is the estimated system frequency response at harmonic k,

(iii) the mean error in the frequency response defined by

$$A_{\text{mean}} = \frac{1}{F}\sum_{k=1}^{F} |\hat{G}(k) - G(k)| \tag{3}$$

where F is the highest specified (excited) harmonic, and

(iv) the maximum error in the frequency response defined by

$$A_{\max} = \max_k (|\hat{G}(k) - G(k)|). \tag{4}$$

The measure D provides an indication of the uncertainty of the estimates. It is important in robust controller design where decisions are guided by the size of the model uncertainty. On the other hand, accuracy of the frequency response is crucial in the design of controllers such as the proportional-integral-derivative controller, where tuning is frequently performed in the frequency domain. The measure that is of prime importance depends on the application.

III. EXPERIMENTAL THERMOSTAT SYSTEM

In this experiment, the ELWE LEHRSYSTEM thermostat system [26] was utilized. The entire system (as shown in Figure 2) has a length of 25.4 cm, a width of 20.3 cm and a height of 30.5 cm. It can accept manual input through an adjustment knob, an internally programmed ramp input, and a user-defined signal from a data acquisition system (DAQ). The system has a proportional-integral controller.

The ELWE LEHRSYSTEM thermostat can accept input signals with two different voltage ranges, which are from -10 V to $+10$ V and -15 V to $+15$ V. In this investigation, the -10 V to $+10$ V range was utilized. The specifications of this thermostat are given below:

- Operating temperature range: 0 °C – 100 °C
- Supply voltage: 230 V

FIGURE 3. Photograph of the experimental set-up.

- Supply current: 0.5 A
- Frequency: 50/60 Hz

Data input and output were performed through a National Instruments (NI) myDAQ device, which is controlled through the NI LabVIEW-based software appliance [27]. It has the combined functions of digital multimeter, oscilloscope, function generator, variable power supply, Bode plot analyzer, dynamic signal analyzer, impedance analyzer, two-wire current-voltage analyzer and three-wire current-voltage analyzer.

In this investigation, the NI myDAQ was applied as an arbitrary waveform (input signal) generator, which provided input voltage to the ELWE LEHRSYSTEM thermostat. Connections to the thermostat were made using probe wires. The NI myDAQ device was connected via a universal serial bus cable to a laptop with LabVIEW software installed. This enabled experimental data to be displayed and stored in the laptop for analysis. A photograph of the experimental set-up is shown in Figure 3.

IV. PRELIMINARY TESTS

Preliminary tests were first conducted to check the significance of nonlinear distortion as well as to obtain suitable values of the sampling time t_s and the measurement time T_N. A positive step test was applied, stepping the input from 0 V to $+10$ V. The output was observed to change from 0 °C to around 100 °C. A negative step test was applied next, stepping the input from $+10$ V to 0 V. The output decreased back to 0 °C. In both cases, the time taken to reach 63% of the total temperature change was found to be around 50 s. The output reached steady state after 250 s. The positive and negative step responses were largely symmetrical, indicating that nonlinear distortion was negligible. Based on the preliminary step tests, the sampling time t_s was set to 5 s, whereas the measurement time T_N was set to 250 s according to the recommendations in [5]. The signal period was calculated using $N = T_N/t_s = 50$.

An initial model, $G_{\text{i}}(z)$, was identified based on the step response tests as

$$G_{\text{i}}(z) = \frac{0.7953}{1 - 1.1218z^{-1} + 0.2013z^{-2}}. \tag{5}$$

Only a low order model could be identified because the step inputs lacked high frequency components and because

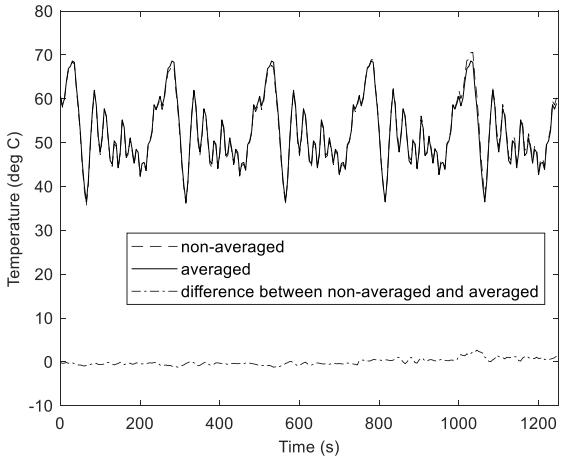

FIGURE 4. Five periods of the measured output.

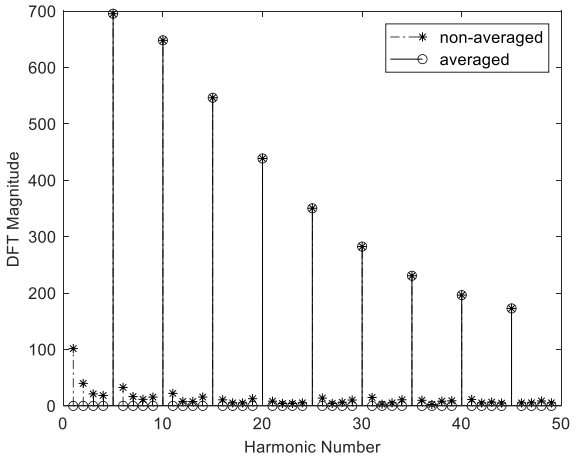

FIGURE 5. DFT magnitudes of the measured output. Only the first 50 harmonics (out of 250 harmonics) are shown for better clarity.

the system suffered from the presence of significant disturbances. $G_{\rm i}(z)$ has a gain of 10. It will be subsequently used in Section VI to design optimal signals, where the parameters of $G_{\rm i}(z)$ will affect the shape of the amplitude spectra of the optimal signals.

V. IDENTIFICATION OF BENCHMARK MODEL

A benchmark model was subsequently obtained by exciting the system with a flat spectrum multisine signal of period $N = 50$ and 20 consecutive excited harmonics (from harmonics 1 to 20). The highest specified harmonic F was set to approximately $0.4N$, according to the recommendation in [5]. The sampling time t_s was set to 5 s based on the preliminary tests. The signal amplitude ranged from 2.96 V to 7.03 V, with a nominal value of 5 V. The flat multisine signal u was fed ten times into the system and the output data of periods 1 to 10 ($y_1, y_2, \ldots, y_{10}$) were measured in synchrony with the input. The last five periods of the output data (y_6 to y_{10}) were averaged to reduce the effects of noise. The SNR was approximately 17 dB, hence justifying the need for averaging in the quest for a benchmark model. Figure 4 depicts the

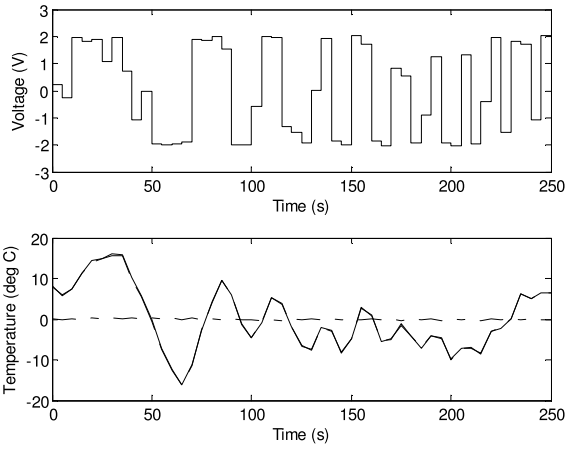

FIGURE 6. Time domain signals with mean removed. Top: input; bottom: output. For the bottom subplot - solid line: measured; dashed line: benchmark model; dashed-dotted line: error.

non-averaged output and the averaged output signals as well as the difference between them.

The effects of averaging can be clearly observed in the frequency domain, as depicted in Figure 5. Taking a 250-point discrete Fourier transform (DFT), contributions of the linear component of the system will appear at harmonics 5, 10, 15, 20, 25, ... These are at multiples of five because five steady state periods were taken. The power at the rest of the harmonics such as harmonics 1, 2, 3, 4, 6, 7, 8, ... can be attributed to the effects of noise [3]. These are non-periodic components and they can be removed via averaging. This will ensure that the resulting benchmark model will have high fidelity since it will be used as a basis for the comparison of different input spectrum designs.

The average of the last five periods of the output data (y_6 to y_{10}) served as the training output for the identification of the benchmark model. The second to fifth periods of the output data (y_2 to y_5) were also averaged; this served as the validation output. The training data and validation data were fed into the System Identification Toolbox [28] in MATLAB. The mean values of the signals were set to zero, as is the typical practice in system identification. Transient effects were removed by discarding the first period (y_1).

The benchmark model order was selected using Akaike's Information Criterion [29]. The Rissanen's Minimum Description Length Criterion [30] also resulted in the same order. The resulting benchmark model, $G_{\rm b}(z)$, is given by

$$G_{\rm b}(z) = \frac{1.839 + 1.344z^{-1} - 1.213z^{-2} - 0.3446z^{-3} - 0.02459z^{-4}}{(1 - 0.7649z^{-1} - 0.5904z^{-2} + 0.6471z^{-3} - 0.2626z^{-4} + 0.1912z^{-5} - 0.06777z^{-6})}. \quad (6)$$

$G_{\rm b}(z)$ has a fit of $100 \times \left(1 - \sqrt{\frac{\sum_n (y(n) - \hat{y}(n))^2}{\sum_n y^2(n)}}\right)\% = 98.47\%$, where n is the discrete time index and $\hat{y}$ denotes the estimated output. $G_{\rm b}(z)$ was identified using the autoregressive with

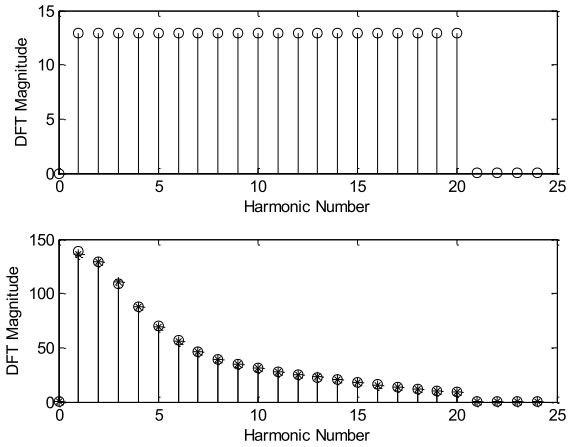

FIGURE 7. DFT magnitudes. Top: input; bottom: output. For the bottom subplot - circles: measured; asterisks: benchmark model.

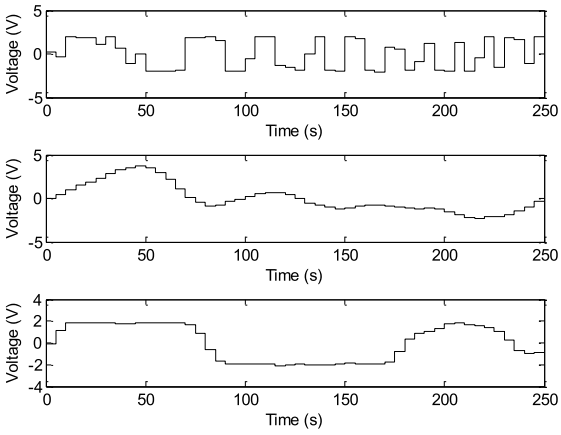

FIGURE 8. Perturbation signals in the time domain. Top: flat; middle: MOOSE2; bottom: optexcit.

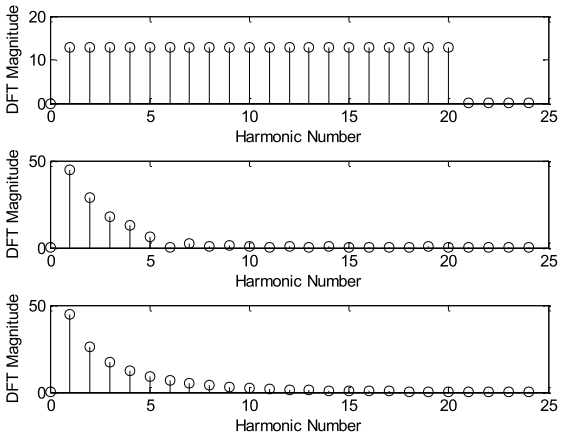

FIGURE 9. Perturbation signals in the frequency domain. Top: flat; middle: MOOSE2; bottom: optexcit.

exogenous input (ARX) model structure; a lower fit was obtained using the output error (OE) model structure. The system gain of $G_b(z)$ is 10.5.

The measured output and the benchmark model output in the time domain are compared in Figure 6. From Figure 6, the benchmark model output matches the measured output very well, with the error being almost zero. In Figure 7, the DFT magnitudes are compared. The trend in the DFT magnitude has been successfully captured by $G_b(z)$. The high accuracy was made possible by the averaging of multiple periods of the input-output data.

VI. COMPARISON OF SIGNAL DESIGNS

Three different spectra were considered, namely the flat spectrum, MOOSE2 spectrum and optexcit spectrum. Perturbation signals with these spectra were implemented using multisine signals of period $N = 50$ and 20 consecutive excited harmonics (from harmonics 1 to 20). The sampling time t_s was set to 5 s based on the preliminary tests. The flat spectrum signal was the same as that used for identifying the benchmark model and it is non-optimized. The MOOSE2 and optexcit signals are optimal signals, and they were designed based on $G_i(z)$ given in (5).

To obtain the MOOSE2 signal, the MOOSE2 program [15], [16], [17] was applied to generate the MOOSE2 spectrum. The MOOSE2 program was set to minimize the determinant of the covariance matrix of the estimated parameters based on the D-optimality criterion. This made the objective function of MOOSE2 as similar as possible to that of optexcit. The MOOSE2 spectrum was parameterized as a transfer function. The flat spectrum signal was passed through this transfer function which works like a shaping filter. The output of the filter gives the MOOSE2 signal.

The optexcit signal was generated by making use of the optexcit algorithm in the FDIDENT Toolbox in MATLAB [18], [19], [20], [21]. The algorithm optimizes the power spectrum of the input signal in the sense that it minimizes the volume of the uncertainty ellipsoid of the estimated parameters. This power spectrum was fed into a time-frequency swapping algorithm [31] to generate the optexcit signal.

The three signals with different spectra were scaled to give the same root-mean-square value of 2.68 V, for fair comparison. The signal and their DFT magnitudes are plotted in Figures 8 and 9, respectively. The signals were fed into the thermostat system in three separate experiments after being shifted by the nominal input voltage of 5 V. In each experiment, transient effects were removed by collecting two periods of the output and discarding the first period. Noise at the non-excited harmonics was filtered to improve the output SNR. The input and output data, with mean values removed, were fed into the System Identification Toolbox in MATLAB. The training set was the same as the validation set as only one period of steady state data was available. The experiment was designed to test the accuracy of the identification under stringent limits on the experiment time.

Two model structures were considered, namely the ARX and OE model structures. Six different models were estimated, which are $G_{FA}(z)$ and $G_{FO}(z)$ obtained using the flat spectrum signal, $G_{MA}(z)$ and $G_{MO}(z)$ obtained using the MOOSE2 signal, and $G_{OA}(z)$ and $G_{OO}(z)$ obtained using the

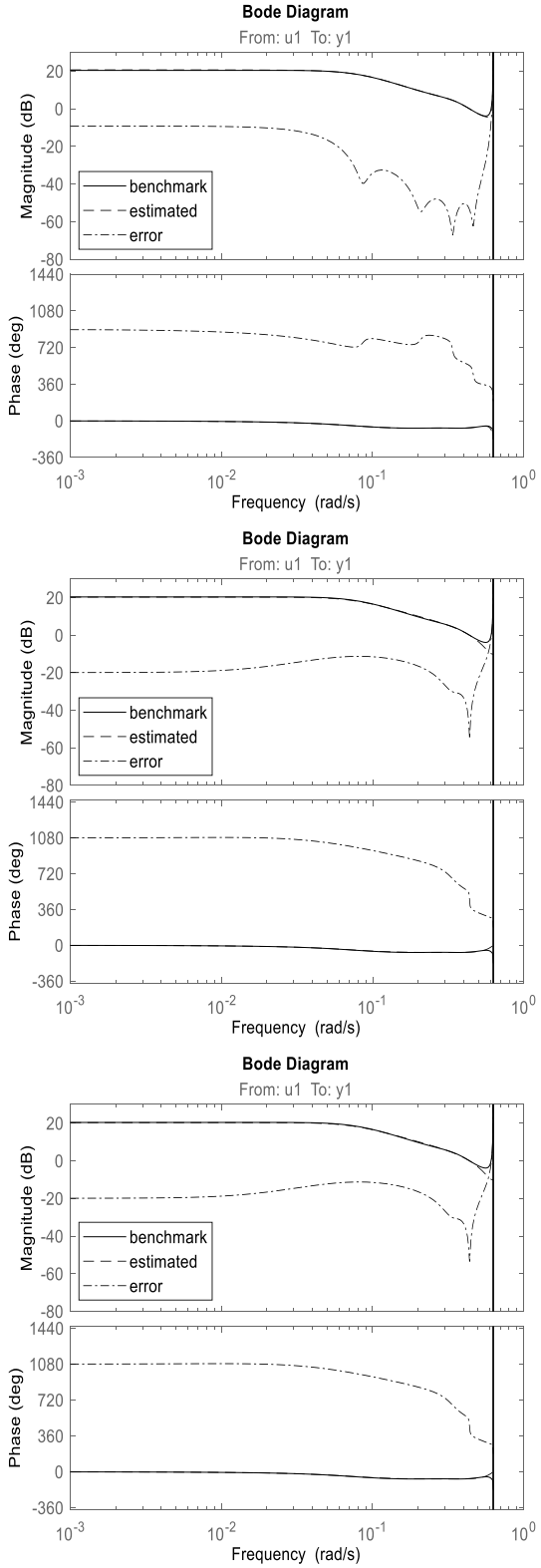

FIGURE 10. Bode plots comparing the benchmark with the estimated models. Top: $G_{FA}(z)$; middle: $G_{MA}(z)$; bottom: $G_{OA}(z)$.

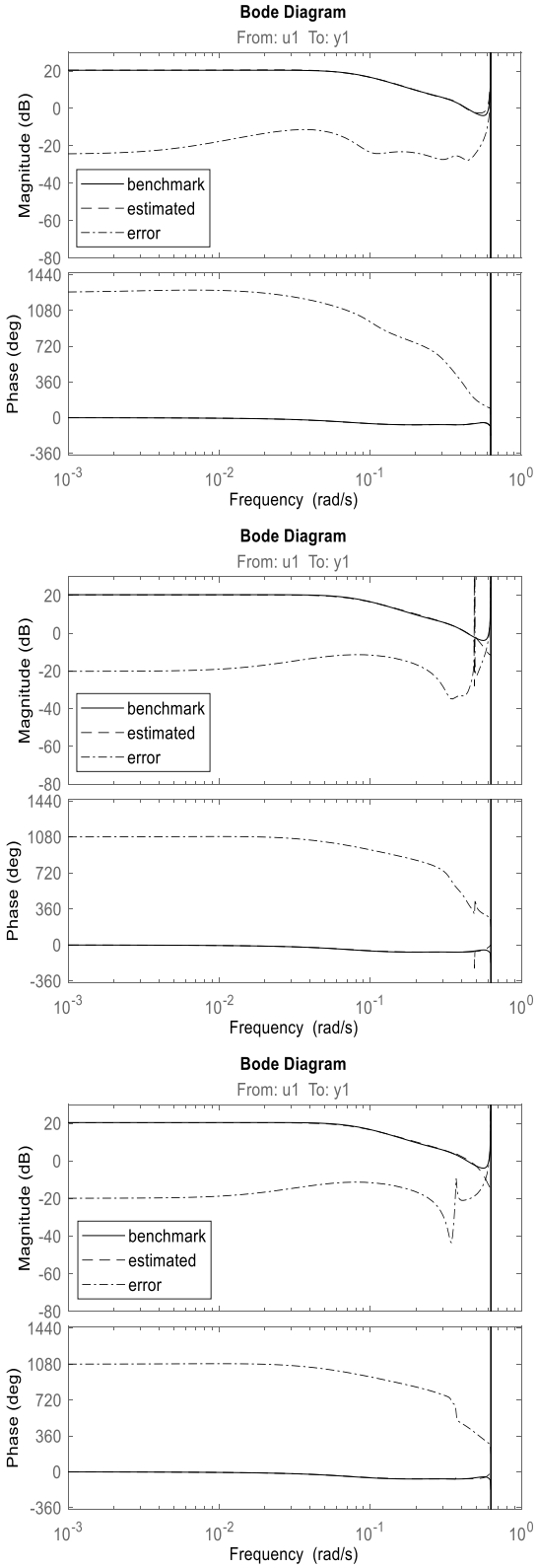

FIGURE 11. Bode plots comparing the benchmark with the estimated models. Top: $G_{FO}(z)$; middle: $G_{MO}(z)$; bottom: $G_{OO}(z)$.

optexcit signal. $G_{FA}(z)$, $G_{MA}(z)$ and $G_{OA}(z)$ are ARX models, whereas $G_{FO}(z)$, $G_{MO}(z)$ and $G_{OO}(z)$ are OE models. The estimated models are (7)–(12), as shown at the bottom of the next page.

The results of the performance comparison are shown in Table 1. For the frequency response measures, the range of the frequencies considered was from 0.025 rad/s to 0.503 rad/s,

TABLE 1. Performance measures for six different estimated models. The smallest value in each column is shown in bold font.

Estimated model	D	$A_{\min}$	A_{mean}	$A_{\max}$
Flat ARX	1.473×10^{-42}	**0.0010**	**0.0283**	0.2894
Flat OE	9.929×10^{-47}	0.0422	0.0779	0.2459
MOOSE2 ARX	$\mathbf{5.425\times10^{-94}}$	0.0079	0.1155	0.2740
MOOSE2 OE	1.336×10^{-61}	0.0182	0.1161	0.2695
optexcit ARX	5.692×10^{-94}	0.0080	0.1145	**0.2340**
optexcit OE	5.325×10^{-66}	0.0121	0.1368	0.2732

corresponding to the range covered by harmonics 1 to 20. The Bode plots are shown in Figures 10 and 11.

In terms of D, the MOOSE2 signal with the ARX model outperformed the other combinations, with optexcit ARX following close behind. The flat spectrum signal resulted in much larger values of D. This means that the uncertainties in the model parameters are much larger than those obtained using the MOOSE2 and optexcit signals. Nevertheless, all the values of D are in fact very small, implying that all six models are rather accurate. The ARX models generally performed better than the OE ones on all performance measures because the ARX model can be solved using least squares, which is more robust compared to the recursive solution for the OE model when the estimated model order is quite high (in this case, 6).

The flat spectrum signal with the ARX model achieved the lowest values of $A_{\min}$ and A_{mean}. However, the optexcit ARX combination led to the smallest $A_{\max}$. This implies that the distribution of the error is more uniform across the frequency range of interest for the optexcit ARX combination, as is evident from Figure 10. Comparing Figures 10 and 11, the different weightings in the cost functions for the ARX and OE model structures led to higher estimation accuracy at the higher frequencies for the ARX models, at the expense of a larger bias at the lower frequencies.

Results from this study show that the combined choice of signal and model structure affects the performance measures in different ways. The best choice is application-dependent. Optimal signals with specially designed spectra are effective in reducing the covariance matrix of the parameter estimates and making the error distribution more uniform. However, the flat spectrum signal remains very effective as a general broadband perturbation signal for system identification.

VII. CONCLUSION

Perturbation signals with three different amplitude spectra corresponding to the flat, MOOSE2 and optexcit designs were tested on a thermostat system. The optimal signals were designed using *a priori* information from an initial model identified through step tests. It was found that the combined choice of signal and model structure can significantly affect the performance measures, and the optimal choice depends on the measure that is of prime importance. The covariance matrix of the parameter estimates and the maximum error in the frequency response can be reduced using optimal signals. The use of optimal signals will be beneficial when the identification results are applied for controller design. Nevertheless, the flat spectrum signal remains very useful as a general broadband perturbation signal for system identification as it provides a good overall fit of the frequency response. For the thermostat system, the ARX model structure outperformed the OE model structure because the estimated model order

$$G_{\text{FA}}(z) = \frac{1.848 + 1.662z^{-1} - 0.5800z^{-2} - 0.1874z^{-3} - 0.01262z^{-4}}{(1 - 0.5908z^{-1} - 0.5163z^{-2} + 0.4387z^{-3} - 0.1882z^{-4} + 0.1454z^{-5} - 0.03711z^{-6})}, \tag{7}$$

$$G_{\text{FO}}(z) = \frac{1.833 + 1.691z^{-1} - 0.7826z^{-2} - 0.6832z^{-3} - 0.6899z^{-4}}{(1 - 0.5884z^{-1} - 0.6134z^{-2} + 0.2858z^{-3} - 0.1886z^{-4} + 0.3669z^{-5} - 0.1325z^{-6})}, \tag{8}$$

$$G_{\text{MA}}(z) = \frac{1.875 + 1.563z^{-1} + 0.7189z^{-2} - 0.3289z^{-3} - 0.4997z^{-4}}{(1 - 0.6219z^{-1} + 0.2137z^{-2} - 0.6075z^{-3} + 0.3130z^{-4} + 0.003562z^{-5} + 0.01934z^{-6})}, \tag{9}$$

$$G_{\text{MO}}(z) = \frac{1.871 + 3.236z^{-1} + 1.627z^{-2} - 0.8734z^{-3} - 0.8129z^{-4}}{(1 + 0.2640z^{-1} - 0.5885z^{-2} - 0.6843z^{-3} + 0.4227z^{-4} + 0.05260z^{-5} + 0.01895z^{-6})}, \tag{10}$$

$$G_{\text{OA}}(z) = \frac{1.875 + 1.090z^{-1} + 0.3457z^{-2} - 0.1856z^{-3} - 0.3799z^{-4}}{(1 - 0.8742z^{-1} + 0.3822z^{-2} - 0.5053z^{-3} + 0.2464z^{-4} + 0.0004366z^{-5} + 0.01466z^{-6})}, \tag{11}$$

$$G_{\text{OO}}(z) = \frac{1.861 + 1.517z^{-1} + 1.217z^{-2} + 0.02236z^{-3} - 0.8698z^{-4}}{(1 - 0.6720z^{-1} + 0.5946z^{-2} - 0.9701z^{-3} + 0.3208z^{-4} + 0.07414z^{-5} + 0.01314z^{-6})}. \tag{12}$$

was quite high. The findings from the current work can be generalized to a wide range of systems since the thermostat system has dynamics that are similar to those of many practical systems. The insights from this work are hence useful for control engineering practice.

Suggestions for future work include amplitude spectrum design of perturbation signals for multivariable and nonlinear systems.

REFERENCES

[1] L. Ljung, "System identification," in *Signal Analysis and Prediction*, A. Procházka, J. Uhlíř, P. W. J. Rayner, and N. G. Kingsbury, Eds. Boston, MA, USA: Birkhäuser, 1998, pp. 163–173.
[2] L. Wang, *Model Predictive Control System Design and Implementation Using MATLAB*. London, U.K.: Springer-Verlag, 2009.
[3] J. Schoukens, R. Pintelon, and Y. Rolain, *Mastering System Identification in 100 Exercises*. Hoboken, NJ, USA: Wiley, 2012.
[4] K. R. Godfrey, A. H. Tan, H. A. Barker, and B. Chong, "A survey of readily accessible perturbation signals for system identification in the frequency domain," *Control Eng. Pract.*, vol. 13, pp. 1391–1402, Nov. 2005.
[5] A. H. Tan and K. R. Godfrey, *Industrial Process Identification: Perturbation Signal Design and Applications*. Cham, Switzerland: Springer, 2019.
[6] L. Ljung, *System Identification Theory for the User*. Upper Saddle River, NJ, USA: Prentice-Hall, 1999.
[7] S. Formentin, A. Karimi, and S. M. Savaresi, "Optimal input design for direct data-driven tuning of model-reference controllers," *Automatica*, vol. 49, no. 6, pp. 1874–1882, Jun. 2013.
[8] H. J. van Waarde, "Beyond persistent excitation: Online experiment design for data-driven modeling and control," *IEEE Control Syst. Lett.*, vol. 6, pp. 319–324, 2022.
[9] C. Jauberthie, L. Denis-Vidal, Q. Li, and Z. Cherfi-Boulanger, "Optimal input design for parameter estimation in a bounded-error context for nonlinear dynamical systems," *Automatica*, vol. 92, pp. 86–91, Jun. 2018.
[10] S. Park, D. Kato, Z. Gima, R. Klein, and S. Moura, "Optimal input design for parameter identification in an electrochemical Li-ion battery model," in *Proc. Annu. Amer. Control Conf. (ACC)*, Jun. 2018, pp. 2300–2305.
[11] H. Nian, M. Li, B. Hu, L. Chen, and Y. Xu, "Design method of multisine signal for broadband impedance measurement," *IEEE J. Emerg. Sel. Topics Power Electron.*, vol. 10, no. 3, pp. 2737–2747, Jun. 2022.
[12] B. Mu and T. Chen, "On input design for regularized LTI system identification: Power-constrained input," *Automatica*, vol. 97, pp. 327–338, Nov. 2018.
[13] Y. Fujimoto, I. Maruta, and T. Sugie, "Input design for kernel-based system identification from the viewpoint of frequency response," *IEEE Trans. Autom. Control*, vol. 63, no. 9, pp. 3075–3082, Sep. 2018.
[14] A. H. Tan, "Online input signal design for kernel-based impulse response estimation," *IEEE Trans. Syst., Man, Cybern. Syst.*, vol. 52, no. 11, pp. 7211–7222, Nov. 2022.
[15] M. Annergren and C. A. Larsson. (2016). *MOOSE2: Model Based Optimal Input Design Toolbox for MATLAB (Version 2): User's Guide*. [Online]. Available: https://www.kth.se/polopoly_fs/1.643297.1600689163!/userguide.pdf
[16] M. Annergren and C. A. Larsson, "MOOSE2—A toolbox for least-costly application-oriented input design," *SoftwareX*, vol. 5, pp. 96–100, Jun. 2016.
[17] M. Annergren, C. A. Larsson, H. Hjalmarsson, X. Bombois, and B. Wahlberg, "Application-oriented input design in system identification: Optimal input design for control [applications of control]," *IEEE Control Syst.*, vol. 37, no. 2, pp. 31–56, Apr. 2017.
[18] J. Schoukens, P. Guillaume, and R. Pintelon, "Design of multisine excitations," in *Proc. Int. Conf. Control*, Edinburgh, U.K., 1991, pp. 638–643.
[19] R. Pintelon and J. Schoukens, *System Identification: A Frequency Domain Approach*. Hoboken, NJ, USA: Wiley, 2012.
[20] I. Kollár, *Frequency Domain System Identification Toolbox for Use With MATLAB*. Natick, MA, USA: MathWorks, 1994.
[21] I. Kollár, R. Pintelon, and J. Schoukens, "Frequency domain system identification toolbox for MATLAB: Improvements and new possibilities," *IFAC Proc. Volumes*, vol. 30, no. 11, pp. 943–946, Jul. 1997.
[22] M. T. Sarker, A. H. Tan, and T. T. V. Yap, "Performance evaluation of iterative signal design for system identification," in *Proc. IEEE Int. Conf. Autom. Control Intell. Syst. (I2CACIS)*, Jun. 2022, pp. 203–208.
[23] M. T. Sarker, A. H. Tan, and T. T. V. Yap, "Amplitude spectrum design for multivariable system identification in open loop," in *Proc. IEEE Int. Conf. Autom. Control Intell. Syst. (I2CACIS)*, Jun. 2022, pp. 107–112.
[24] D. Bienvenido-Huertas, "Influence of the type of thermostat on the energy saving obtained with adaptive setpoint temperatures: Analysis in the current and future scenario," *Energy Buildings*, vol. 244, Aug. 2021, Art. no. 111024.
[25] K. C. Chook and A. H. Tan, "Identification of an electric resistance furnace," *IEEE Trans. Instrum. Meas.*, vol. 56, no. 6, pp. 2262–2270, Dec. 2007.
[26] *ELWE LEHRSYSTEM Thermostat 10 13 002*, ELWE, Cremlingen, Germany, 2000.
[27] *NI myDAQ User Guide and Specifications*, National Instruments, Austin, TX, USA, 2016.
[28] L. Ljung, *System Identification Toolbox for Use With MATLAB*. Natick, MA, USA: MathWorks, 1997.
[29] S. Portet, "A primer on model selection using the Akaike information criterion," *Infectious Disease Model.*, vol. 5, pp. 111–128, Jan. 2020.
[30] M. Kawakita and J. Takeuchi, "Minimum description length principle in supervised learning with application to lasso," *IEEE Trans. Inf. Theory*, vol. 66, no. 7, pp. 4245–4269, Jul. 2020.
[31] E. Van der Ouderaa, J. Schoukens, and J. Renneboog, "Peak factor minimization using a time-frequency domain swapping algorithm," *IEEE Trans. Instrum. Meas.*, vol. 37, no. 1, pp. 145–147, Mar. 1988.

MD. TANJIL SARKER received the B.Sc. degree in electrical and electronics engineering (EEE), the Master of Business Administration (MBA) degree in human resource management (HRM) from Bangladesh University, Dhaka, Bangladesh, in 2013 and 2015, respectively, the M.Sc. degree in computer science and engineering (CSE) from Jagannath University, Dhaka, in 2018, and the Ph.D. degree in engineering from the Faculty of Engineering, Multimedia University, Malaysia, in 2022. He has conducted many research works in relevant fields. His research interests include system identification, signal processing and control, renewable energy, power system analysis, and high voltage engineering. He was a Graduate Student Member of the IEEE Student Branch of the Malaysia Section, in 2021.

AI HUI TAN received the B.Eng. degree (Hons.) in electronic engineering, and the Ph.D. degree from the University of Warwick, U.K., in 1999 and 2022, respectively.

She was a consultant at Agilent Technologies, from 2012 to 2013. She joined the Faculty of Engineering, Multimedia University, Cyberjaya, Malaysia, in 2002, where she is currently a Professor. She authored the book *Industrial Process Identification: Perturbation Signal Design and Applications*, which was published by Springer, in 2019. Her research interests include system identification and signal processing.

Prof. Tan has served as a member for the International Federation of Automatic Control (IFAC) Technical Committee on Modeling, Identification and Signal Processing, since 2005. She is a Chartered Engineer registered with the Engineering Council, U.K.

TIMOTHY TZEN VUN YAP received the B.Eng. degree (Hons.) in electronics majoring in computer from Multimedia University, Malaysia, in 2002, and the M.Eng.Sc. and Ph.D. degrees from the System Identification and Control Group, Multimedia University, in 2006 and 2017, respectively. He is currently a Senior Lecturer with the Faculty of Computing and Informatics, Multimedia University. He is also the Chair of the Center for Big Data and Blockchain Technologies, Multimedia University. His current research interests include system identification, blockchain, data engineering, and machine learning.